Masks for alternative X-ray imaging

David Jurado

APLICACIONES INTERDISCIPLINARIAS DE DETECTORES DE PARTÍCULAS

Universidad de los Andes

Conventional X-ray imaging relies on the absorption of X-rays by different tissues, which can result in low-contrast images. A solution to this issue is detecting DPC and DF due to interactions of photons with matter, which is highly sensitive for low-attenuating tissues and samples.

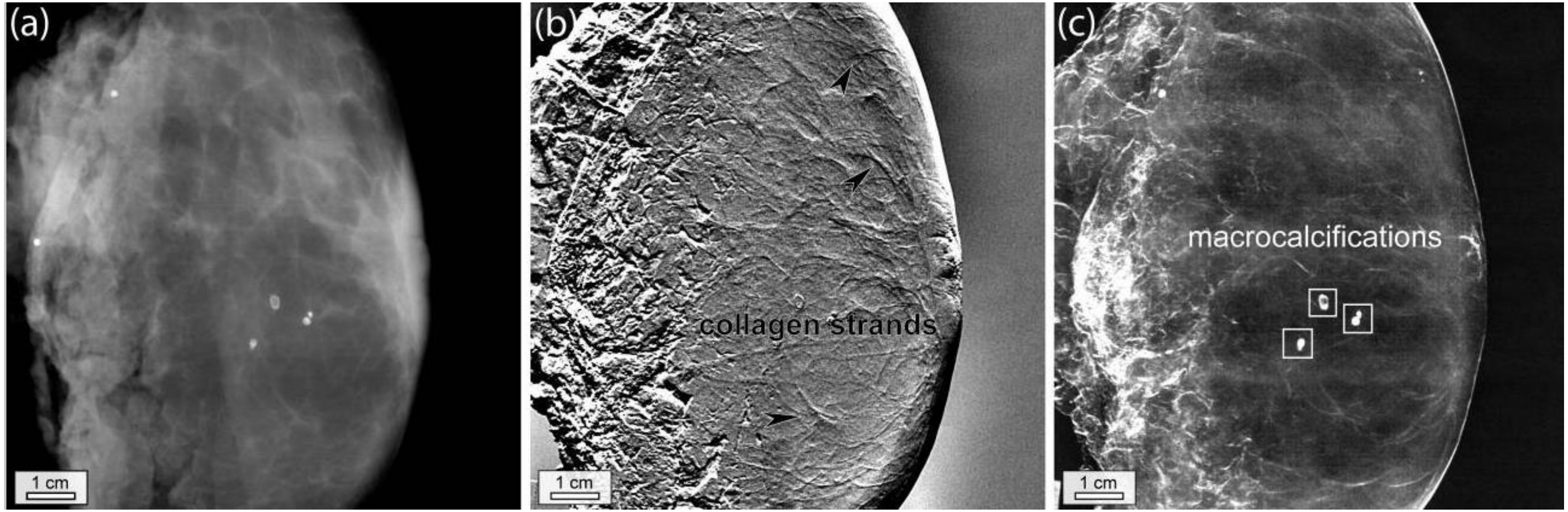

[1]

IT IS CRUCIAL TO MAKE ALTERNATIVE X RAY IMAGING ACCESSIBLE

Light transport approach

Based on [2], The X-ray Fokker-Planck equation is a modified versión of the Transport of Intensity Equation

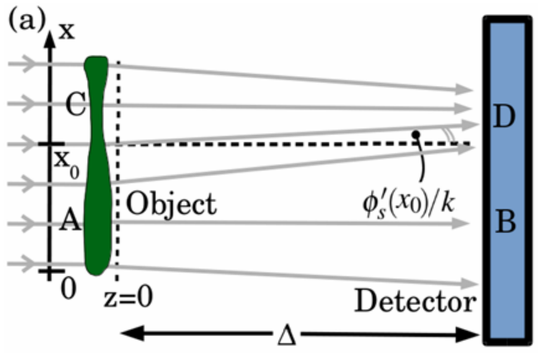

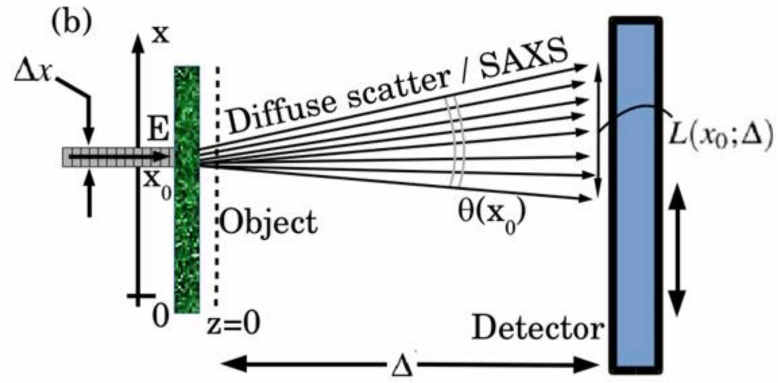

Second order (below the detector resolution)

$$\mathcal{J}_\perp = \mathcal{J}_\perp^{(1)} + \mathcal{J}_\perp^{(2)}$$

$$\mathcal{J}_\perp^{(1)} = \frac{I\nabla_\perp \phi}{k}$$

Transverse Poynting vector

$$\mathcal{J}_\perp^{(2)} = -\nabla_\perp (D\, I)$$

Diffusive energy transport

$$\mathcal{J}_\perp = [1 - F(\boldsymbol{r})]\mathcal{J}_\perp^{(1)} + F(\boldsymbol{r})\mathcal{J}_\perp^{(2)}$$

$$\frac{\partial I}{\partial z} = -\nabla_\perp \cdot \mathcal{J}_\perp \qquad \frac{\partial I}{\partial z} = -\nabla_\perp \cdot [1 - F(\boldsymbol{r})]\mathcal{J}_\perp^{(1)} + F(\boldsymbol{r})\mathcal{J}_\perp^{(2)}$$

Since the fraction of energy converted to small angle scattering in X-rays $F(\boldsymbol{r}) \ll \mathbf{1}$

Then $1 - F(\boldsymbol{r}) \approx 1$

$$\frac{\partial I}{\partial z} = -\nabla_\perp \cdot \left[\frac{I\,\nabla_\perp \phi}{k} - F\nabla_\perp(DI)\right]$$

F varies slowly enough so $\nabla_\perp \cdot [F\nabla_\perp(DI)] \approx F\nabla_\perp^2(DI)$ Yielding the Fokker-Planck equation

$$\frac{\partial I(x,y,z)}{\partial z} = -\nabla_\perp \cdot \left[\frac{I(x,y,z)\nabla_\perp \phi(x,y,z)}{k}\right] - F(x,y,z)\nabla_\perp^2\big(D(x,y,z)I(x,y,z)\big)$$

For a small propagation distance $$I(r,z) = I(r,0) + z\left.\frac{\partial I}{\partial z}\right|_{z=0}$$

$$I(\boldsymbol{r},z) = I(\boldsymbol{r},0) - \frac{z}{k}\nabla_{\perp}\cdot\left(I(\boldsymbol{r},0)\nabla_{\perp}\phi(\boldsymbol{r},0)\right) + z\,F(\boldsymbol{r})D(\boldsymbol{r})\nabla_{\perp}^{2}I(r,0)$$

Given $S(\boldsymbol{r}) = F(\boldsymbol{r})\,D(\boldsymbol{r})$ as the sample scattering coefficient and the setup intensity as $I(r,0) = T(\boldsymbol{r})\,M(\boldsymbol{r})$ Then the measured intensity for a pixel detector is

$$I = \int_A I(\boldsymbol{a},z)\,da$$

For a single row this is:

$$I_n = T(x_n)\int_{x_n}^{x_{n+1}} M(x)\,dx - \frac{z}{k}\,T(x_n)\nabla_{\perp}^{2}\phi(x_n)\int_{x_n}^{x_{n+1}} M(x)\,dx - \frac{z}{k}\,T(x_n)\partial_x\phi(x_n)\int_{x_n}^{x_{n+1}} M'^{(x)}\,dx + zT(x_n)S(x_n)\int_{x_n}^{x_{n+1}} M'^{(x)}\,dx$$

Then $T_n = T(x_n)$, $D_n = \frac{z}{k}\partial_x \phi(x_n)$ and $L_n = \frac{z}{k}\nabla_\perp^2 \phi(x_n)$

$$I_n = T_n \int_{x_n}^{x_{n+1}} M(x)\,dx - T_n L_n \int_{x_n}^{x_{n+1}} M(x)\,dx - T_n\, D_n \int_{x_n}^{x_{n+1}} M'^{(x)}\,dx + z\, T_n\, S(x_n) \int_{x_n}^{x_{n+1}} M''^{(x)}\,dx$$

$$I_n = T_n \int_{x_n}^{x_{n+1}} M(x)\,dx(1 - L_n) - T_n\, D_n \int_{x_n}^{x_{n+1}} M'^{(x)}\,dx + z\, T_n\, S_n \int_{x_n}^{x_{n+1}} M''^{(x)}\,dx$$

Now defining $\int_{x_n}^{x_{n+1}} M(x)\,dx = \mathcal{M}_n$, $\int_{x_n}^{x_{n+1}} M'(x)\,dx = \mathcal{M}_n'$ and $z\int_{x_n}^{x_{n+1}} M''(x)\,dx = \mathcal{M}_n''$

$$I_n = T_n(1 - L_n)\mathcal{M}_n - T_n\, D_n \mathcal{M}_n{}' + T_n\, S_n \mathcal{M}_n{}''$$

Where $\mathcal{M}_n, \mathcal{M}_n', \mathcal{M}_n{}''$ are functions that depends on alignment, mask properties and wavefront markers.

Takeaways:

Laplacian phase correction | Differential phase | Dark field USAXS

$$I_n = \mathcal{M}_n \; T_n(1 - \; L_n) - \mathcal{M}_n' \;\; T_n \, D_n + \mathcal{M}_n'' \, T_n \, S_n$$

Absorption channel | DPC channel | DF channel

$\mathcal{M}_n$ Is the sensibility of each channel in the image

Each column I_n acts like a bin for each signal, retrieval methods can then be used to extract each signal.

Edge Illumination Phase Contrast Imaging

Edge Illumination Phase Contrast Imaging

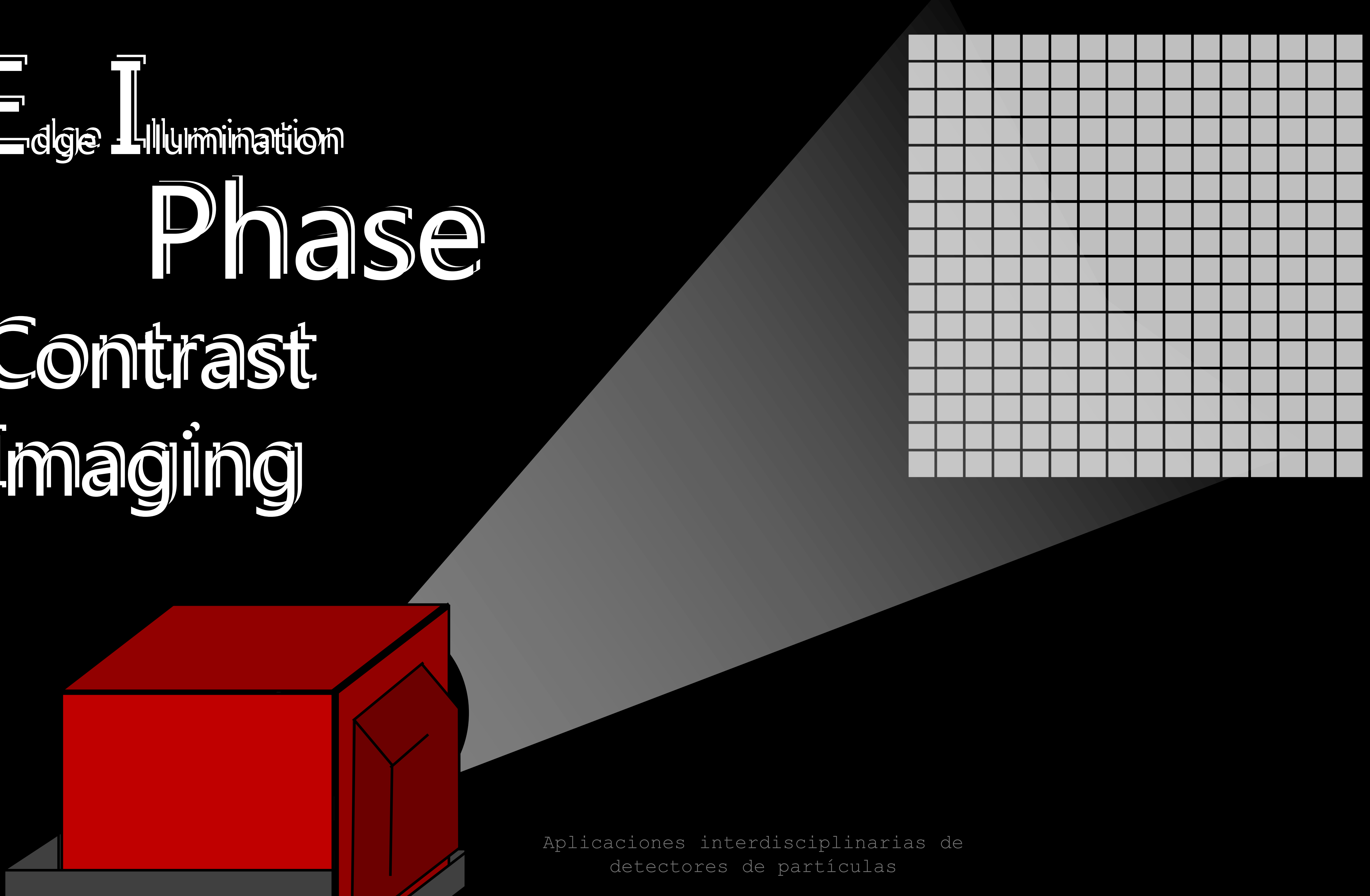

Edge Illumination Phase Contrast Imaging

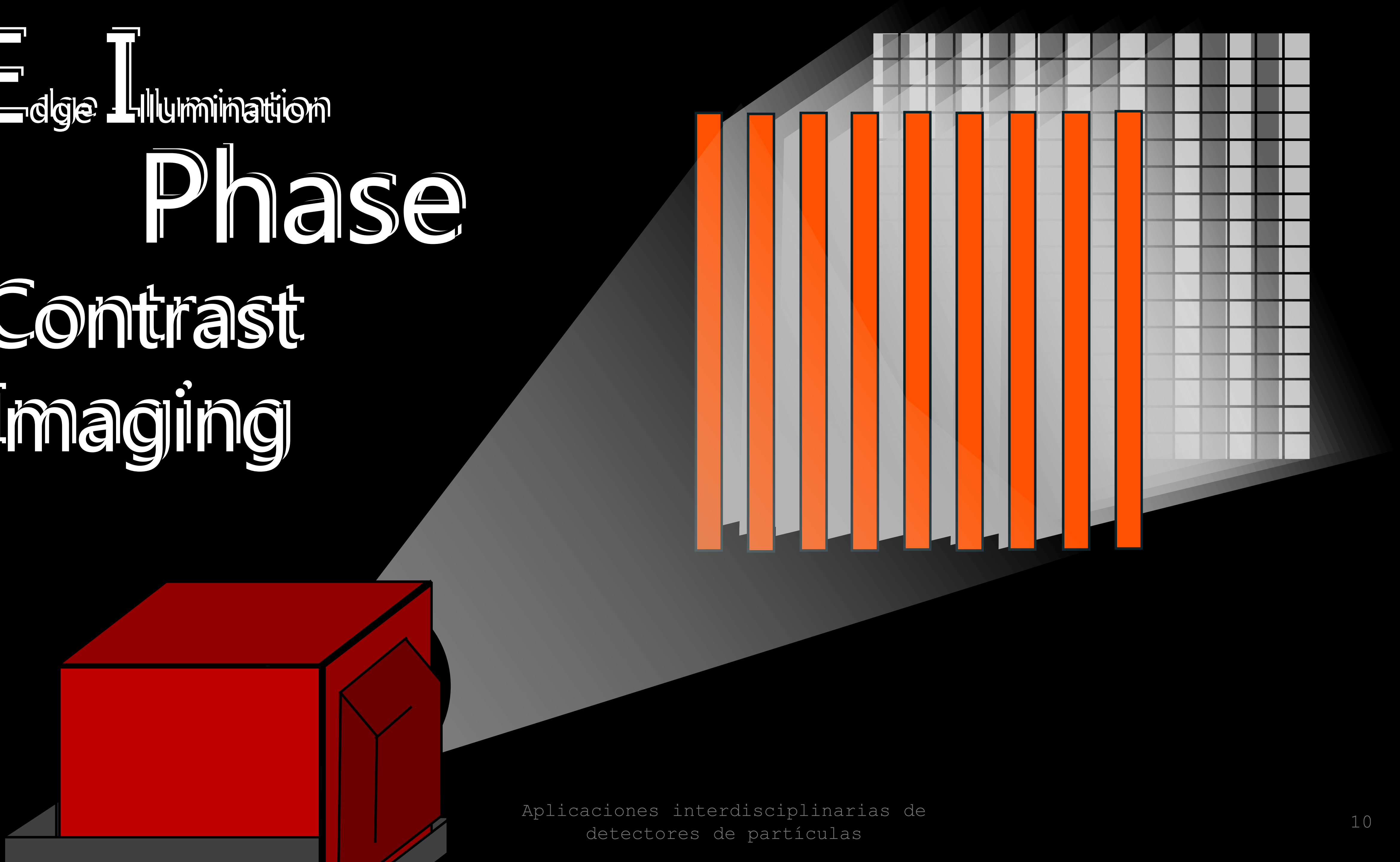

Edge Illumination Phase Contrast Imaging

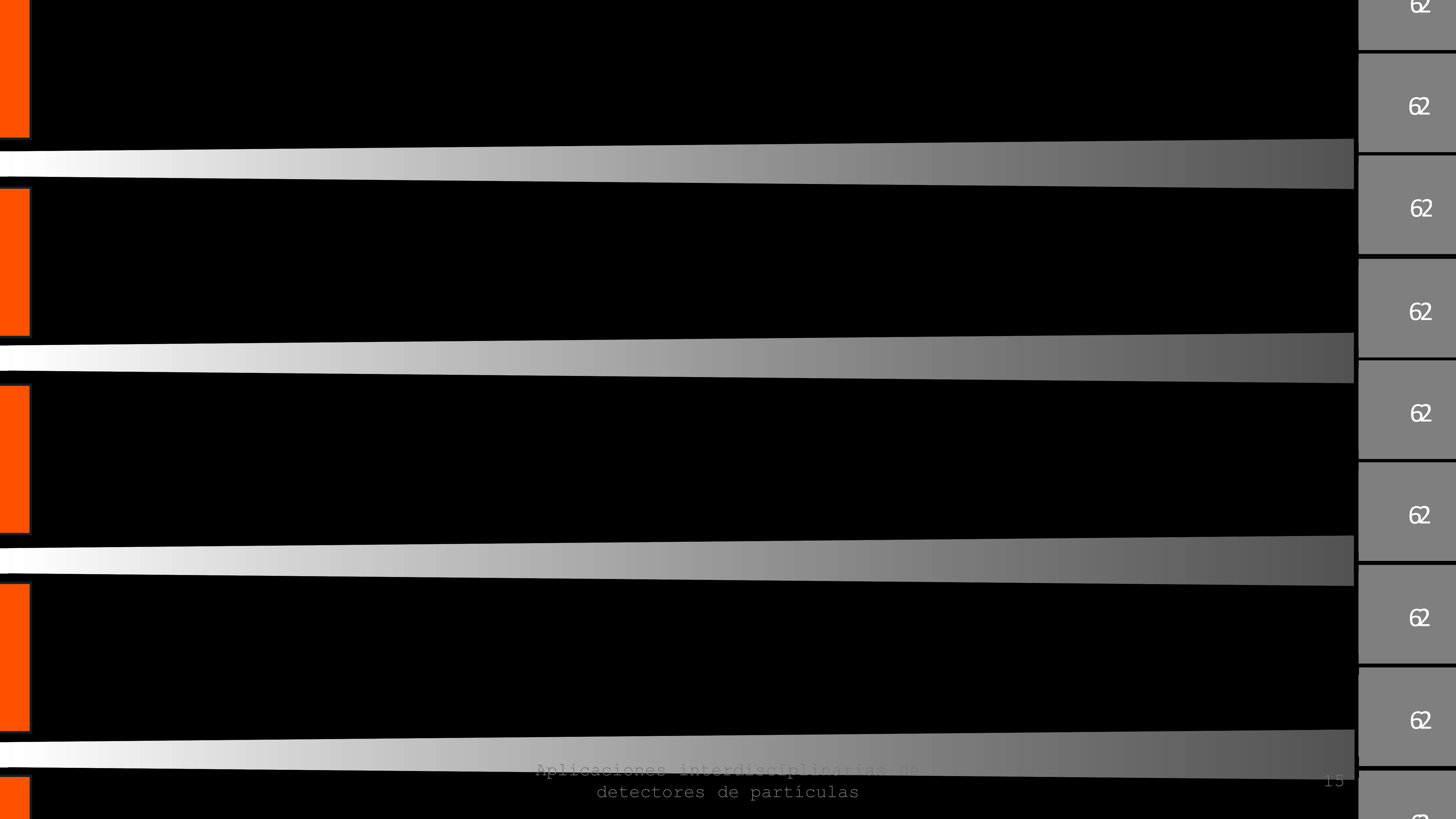
62
62
62
62
62
62
62
62

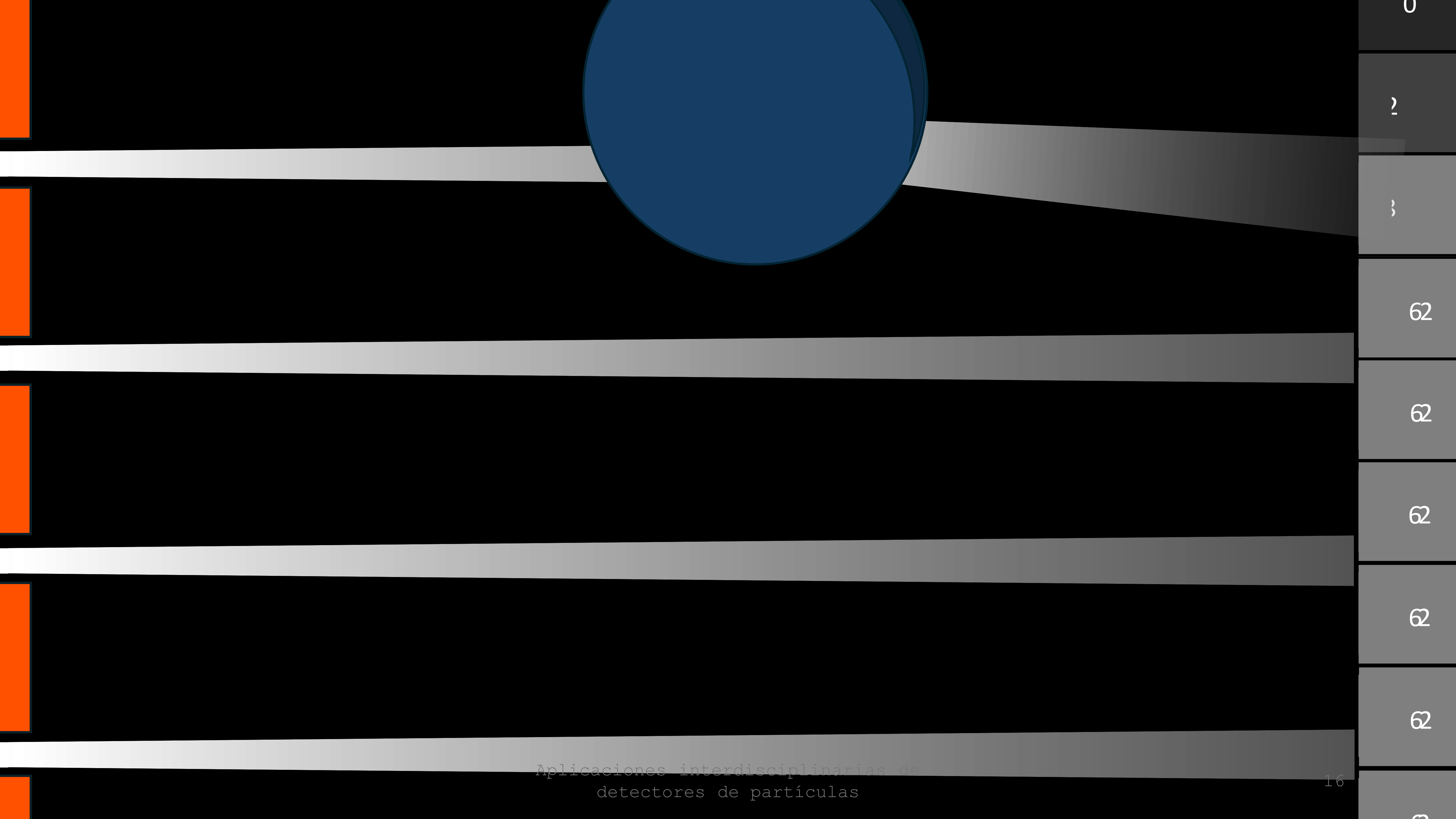
62
62
62
62
62

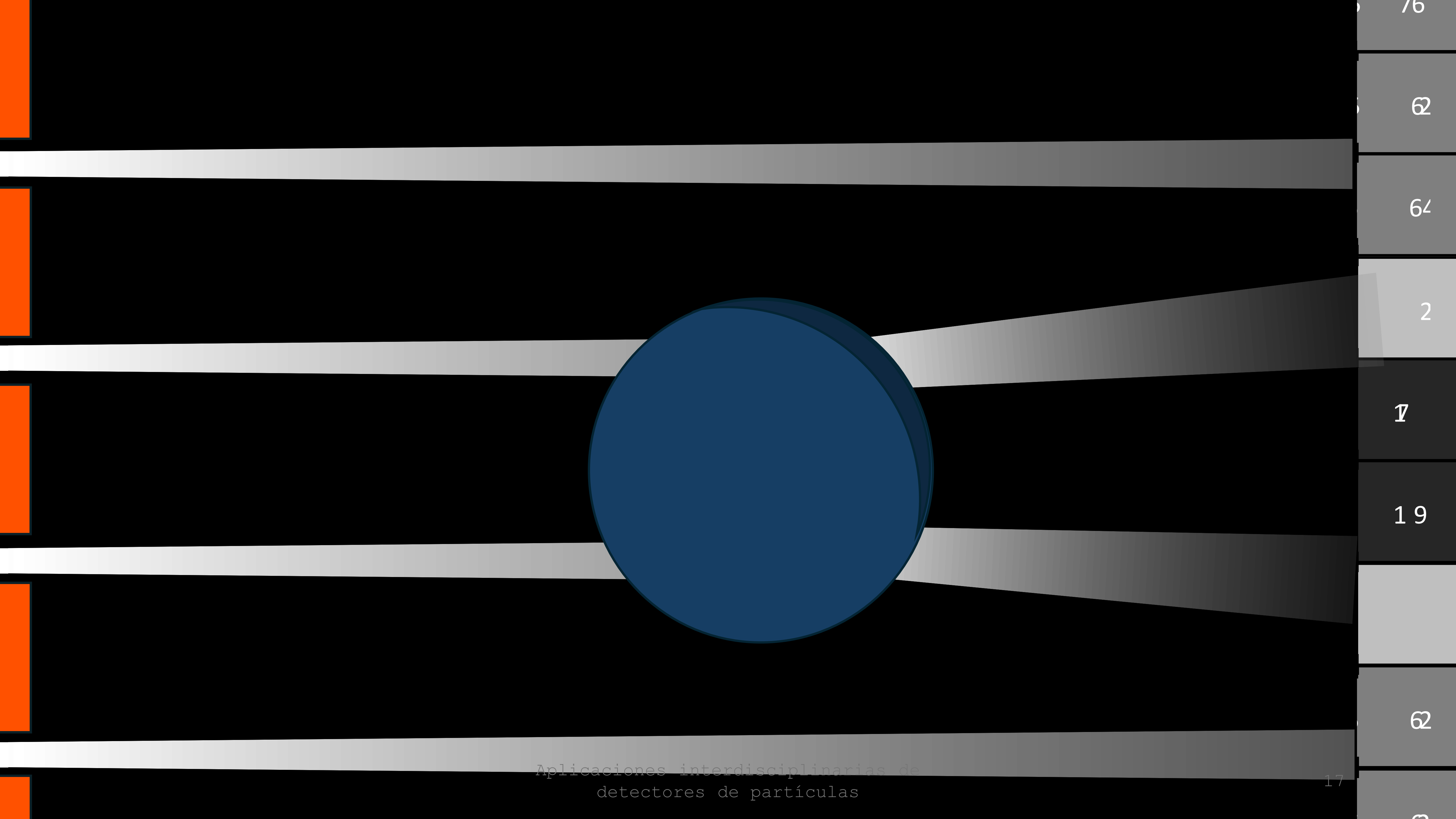
62
2
19
62

62

64

2

76

6

8

62

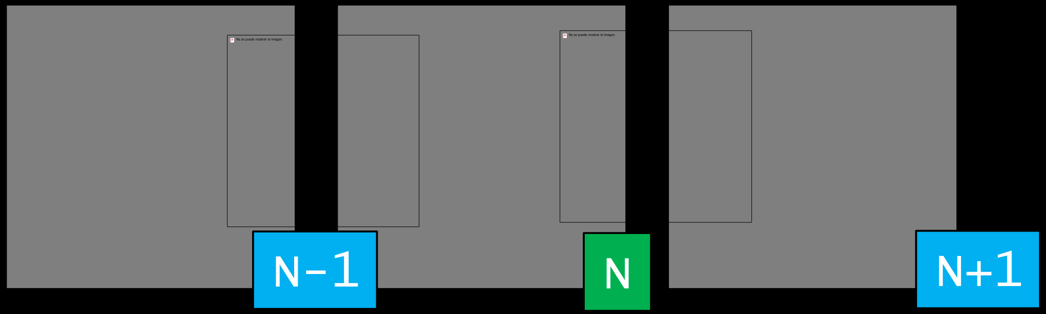
N-1
N
N+1

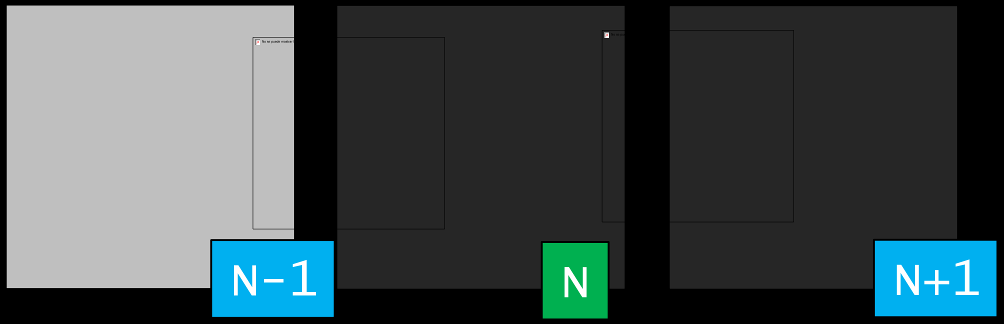
N-1
N
N+1

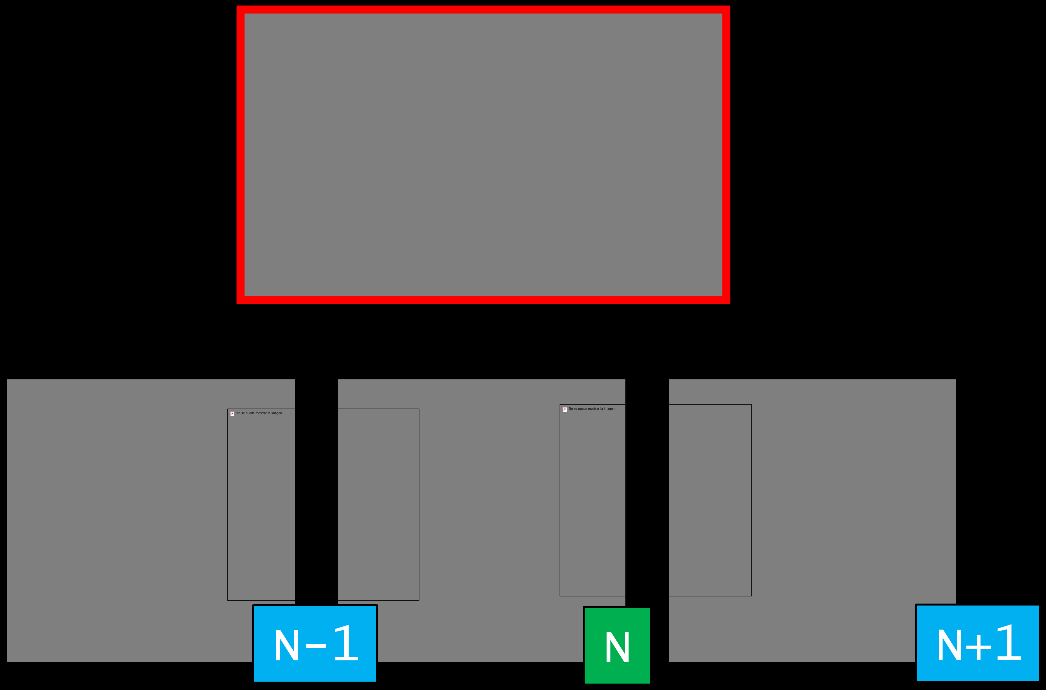
N-1
N
N+1

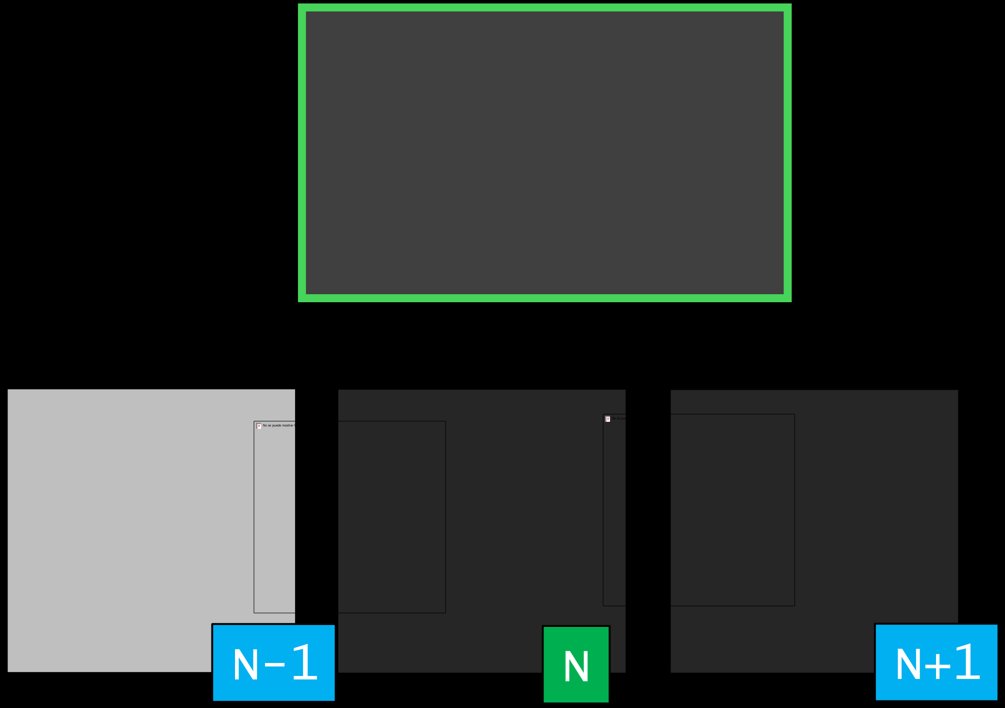
N-1
N
N+1

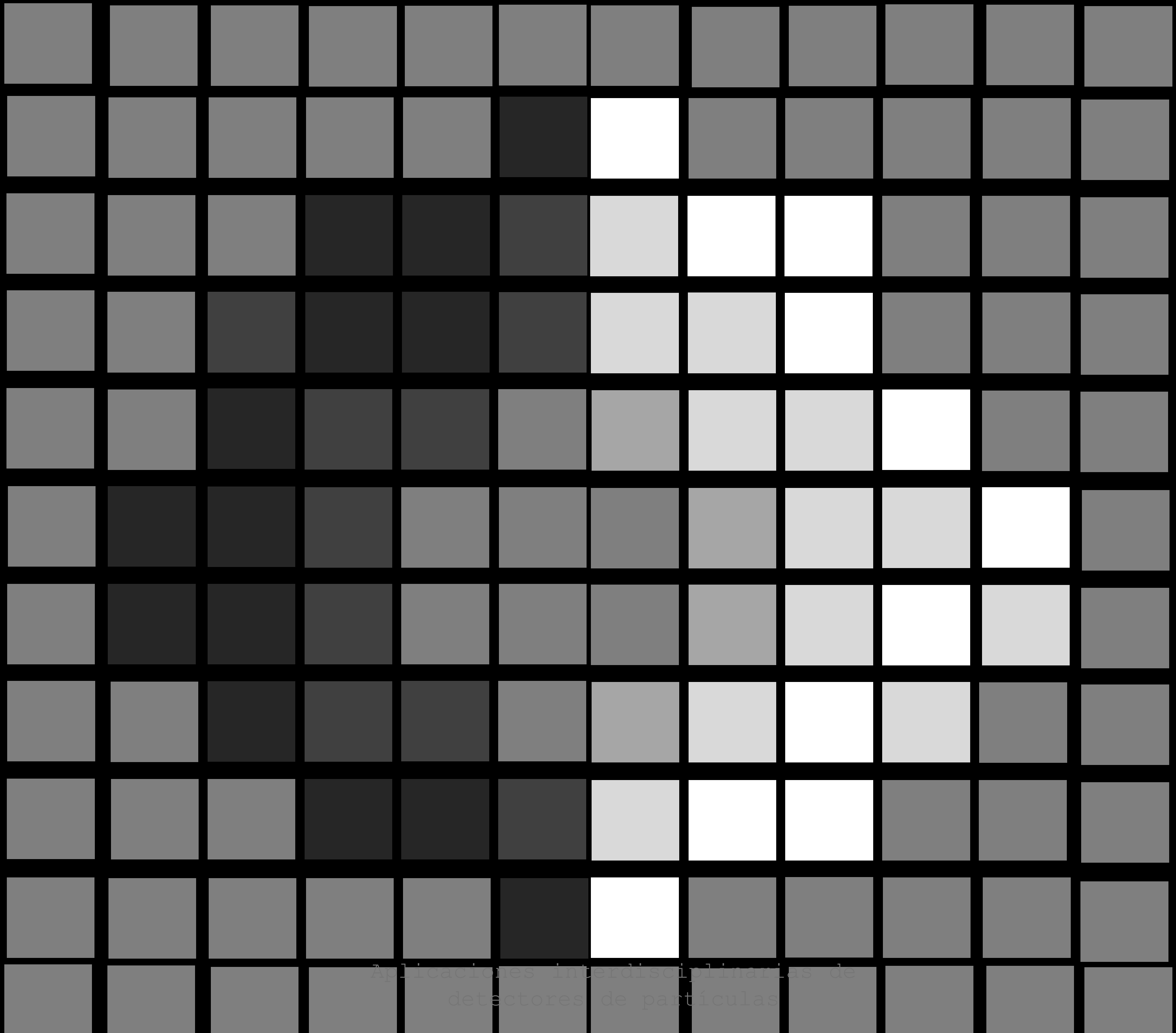

Can we make this technology:

Universal Affordable

Universal

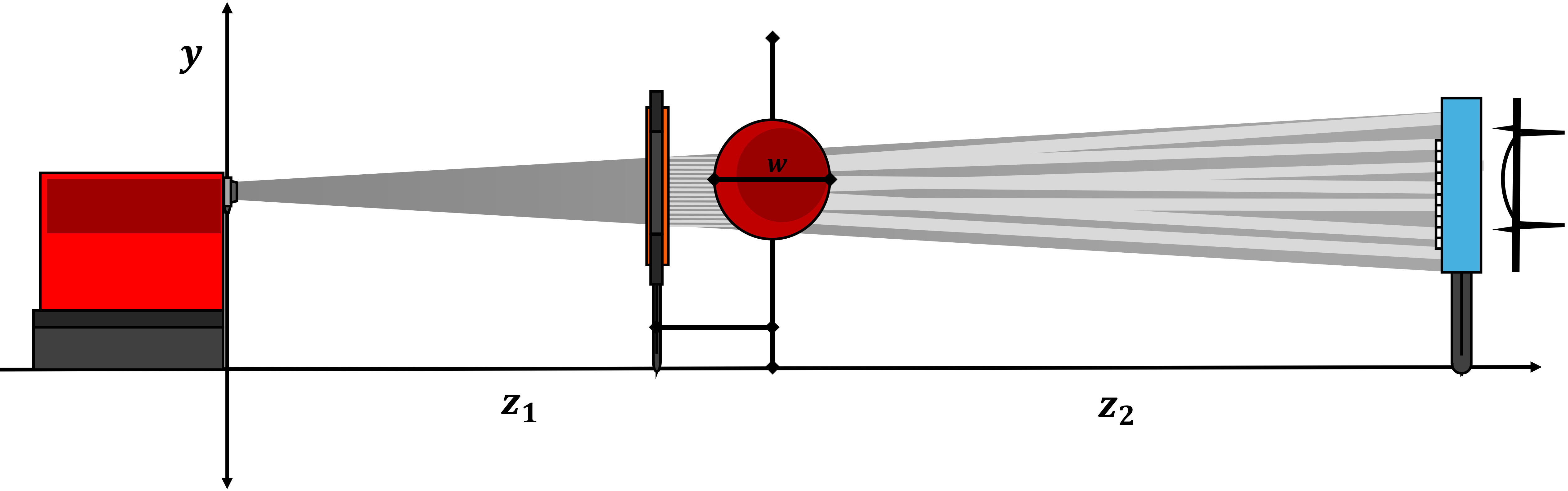

Universal

How do we apply this technique to any X-ray optical setup

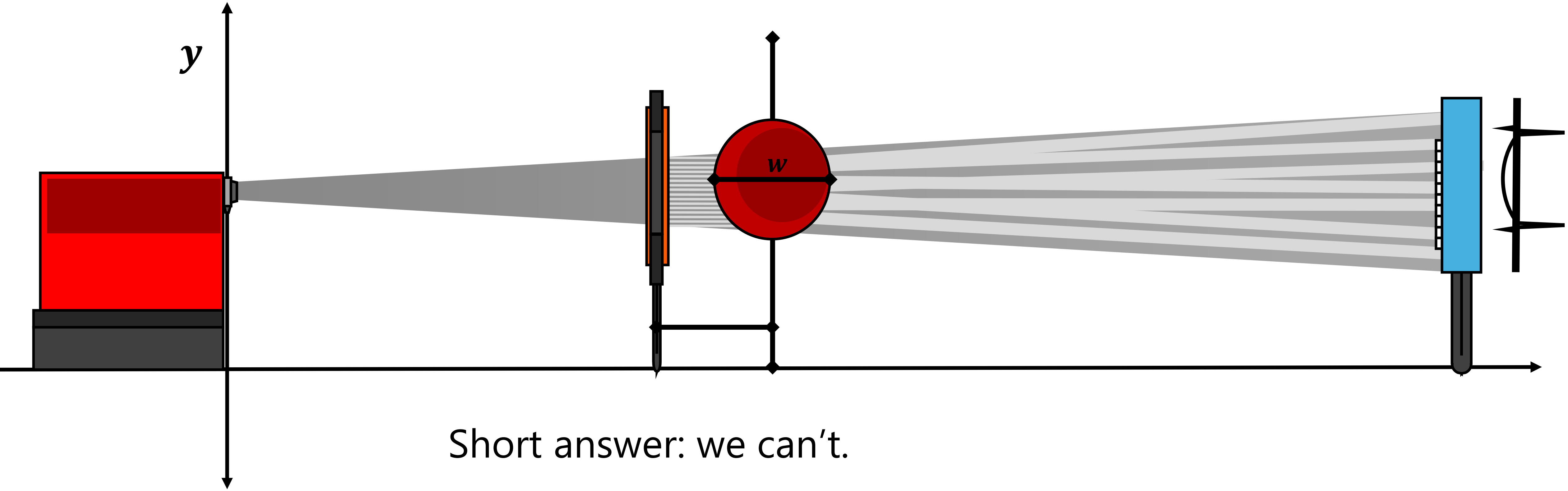

Short answer: we can't.

Universal

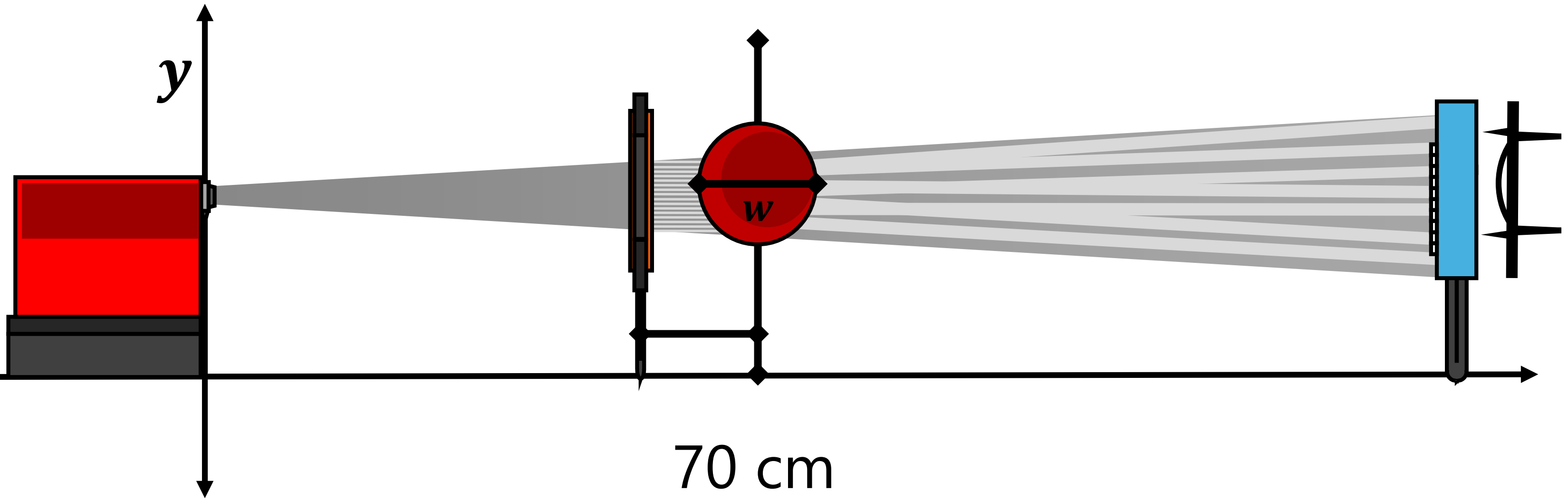

Universal

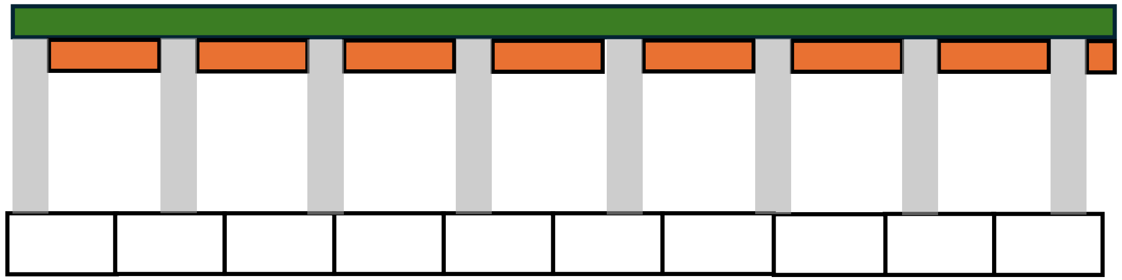

The wavefront marker must match detector pixel distribution given detector and distance (magnification) restrictions

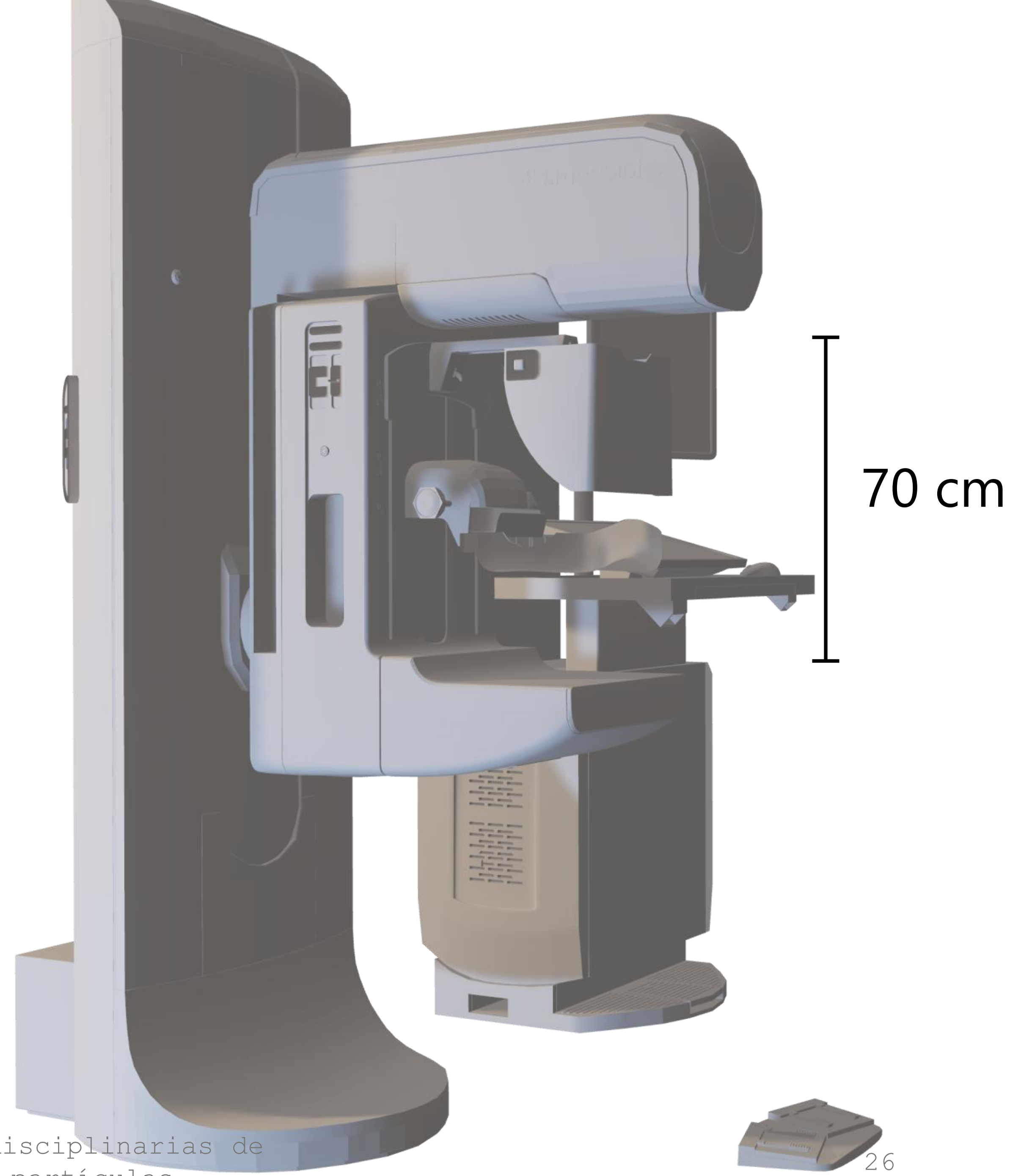

Universal

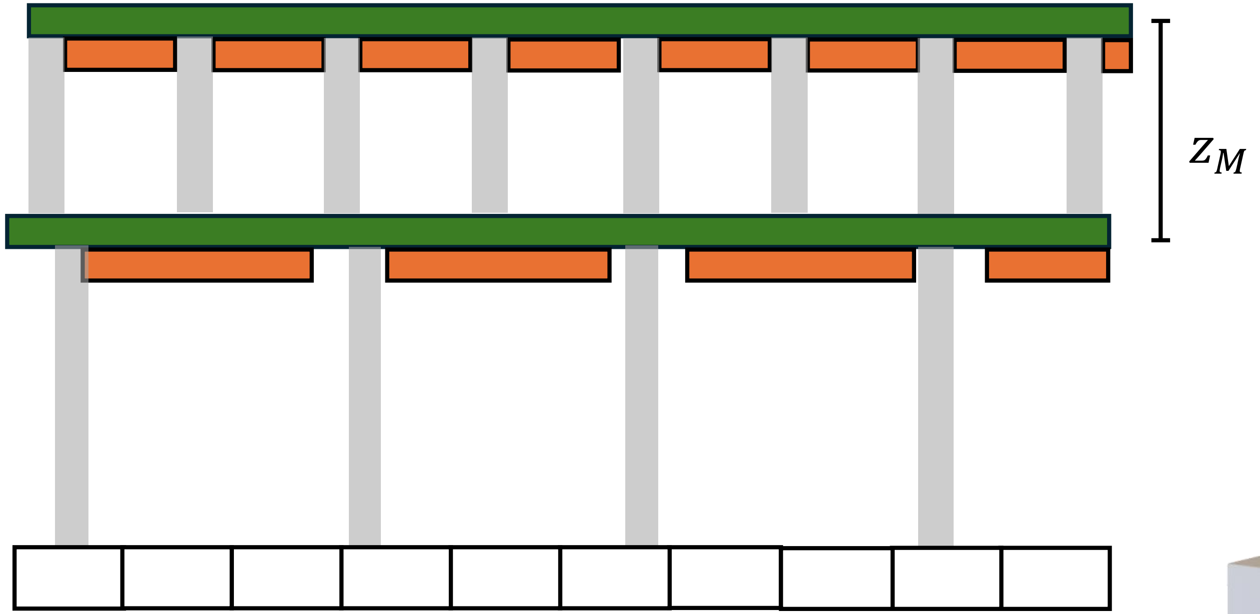

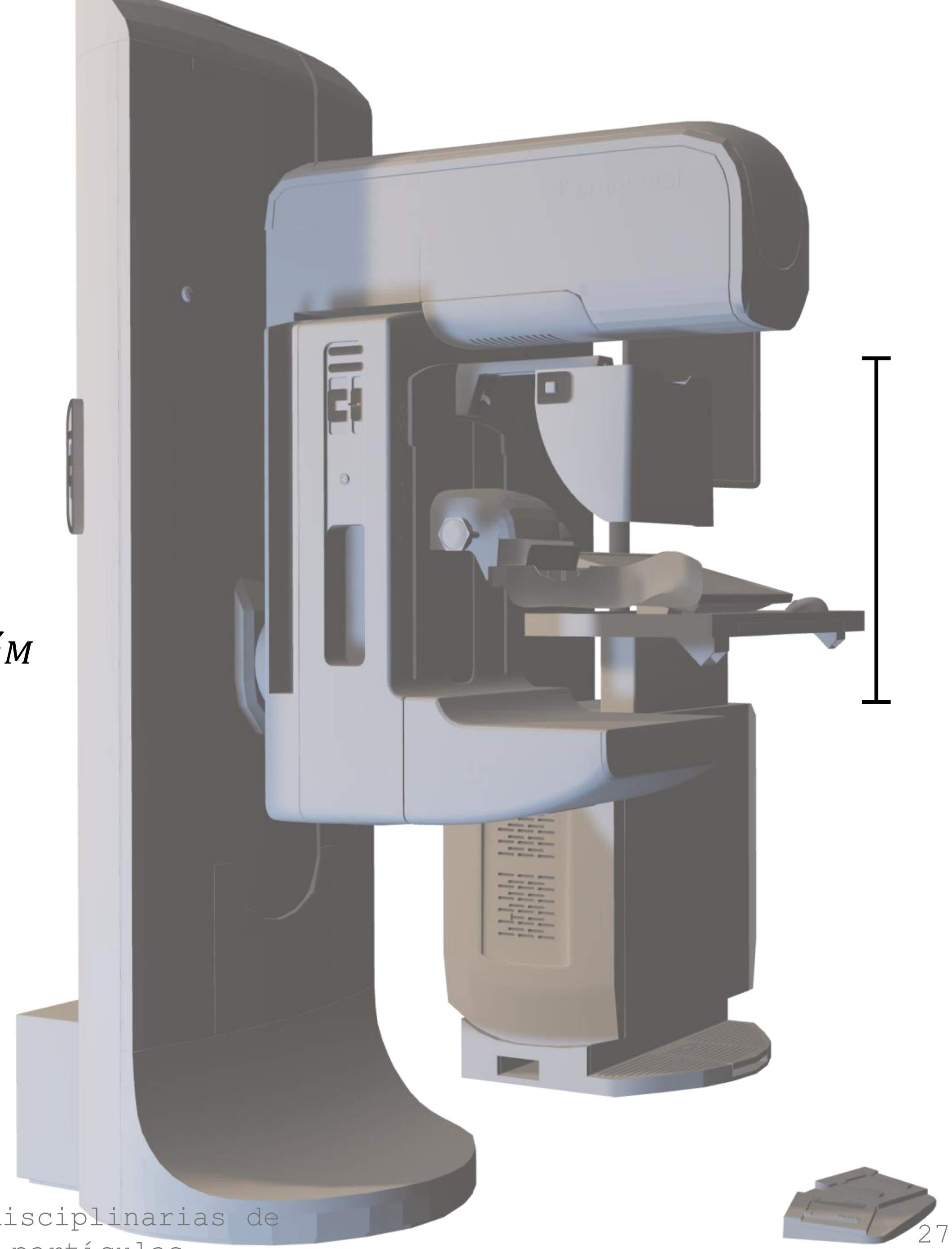

Universal

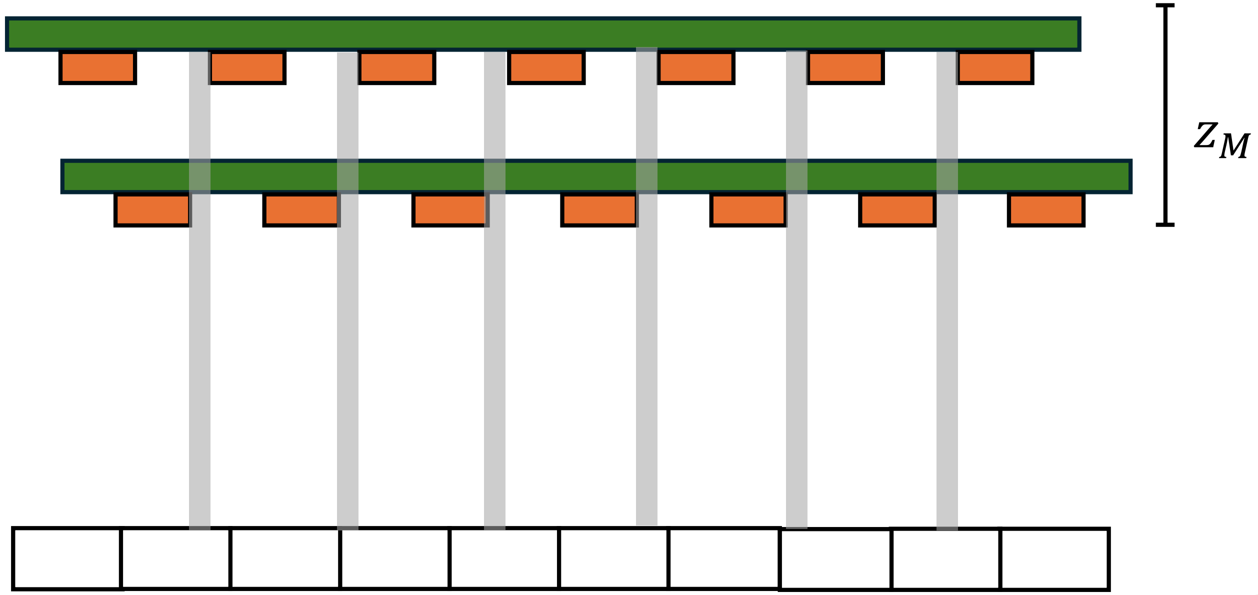

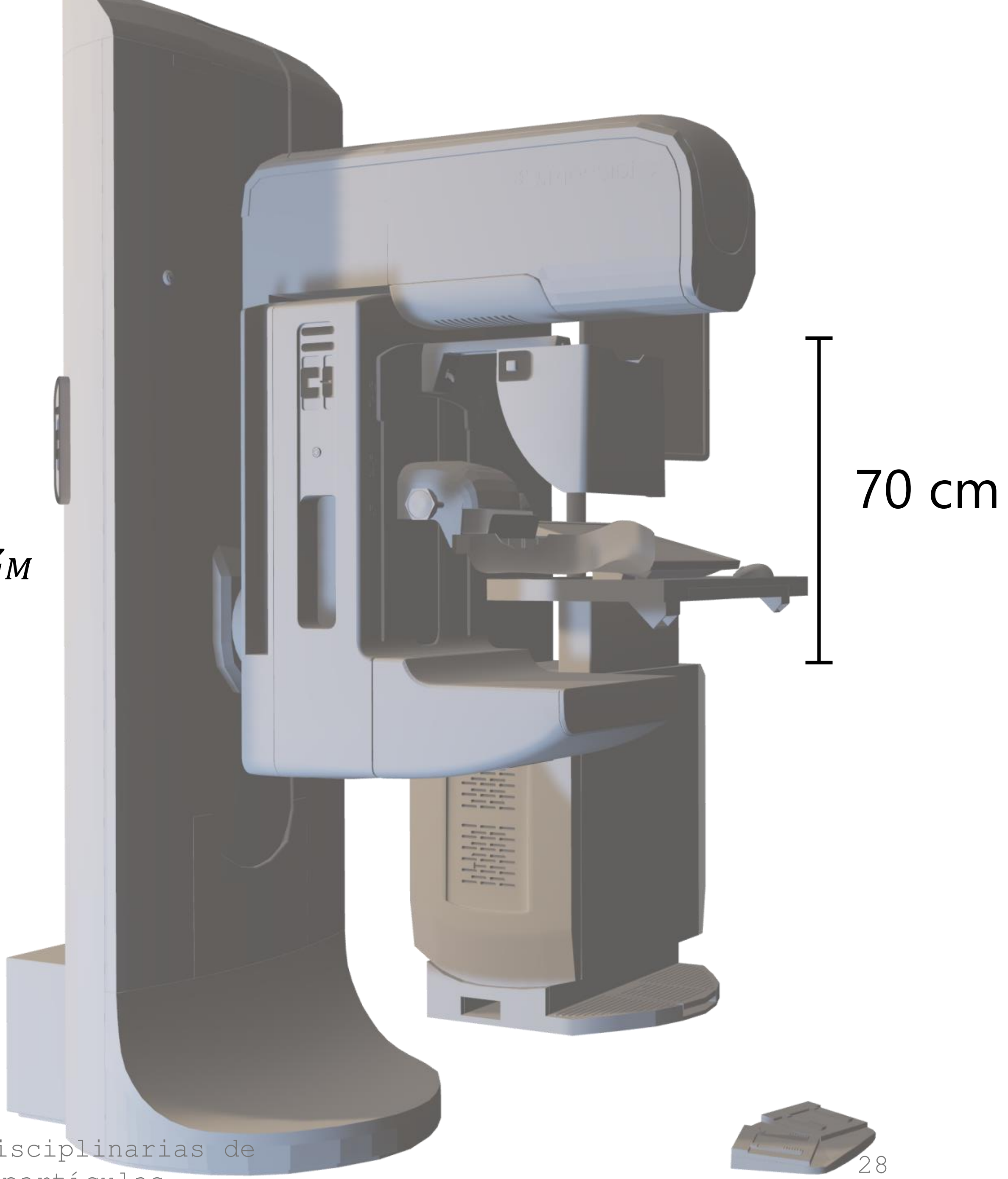

Universal

As long as $z_M \ll z_{s-d}$ the wavefront markers can be operated as a single wavefront marker

$$M_1 \ * M_2 \ * \ \ldots * M_n = \mathcal{M}$$

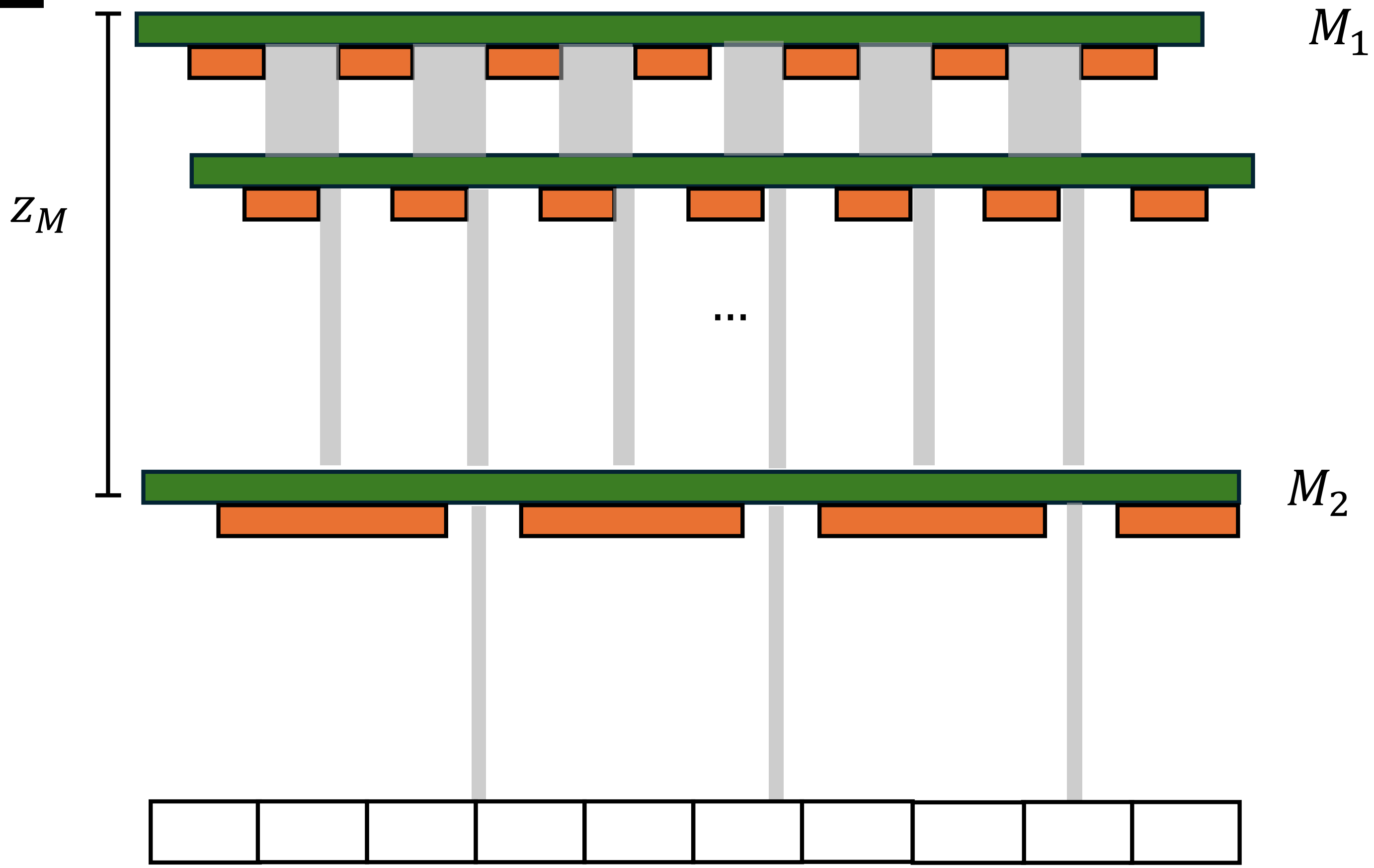

$$T = Max(T_1 . T_2)$$

Affordable

Photolythography

Top quality material, maximizes DF-DPC sensibility

Sub-pixel resolution for most detectors

Few imperfections

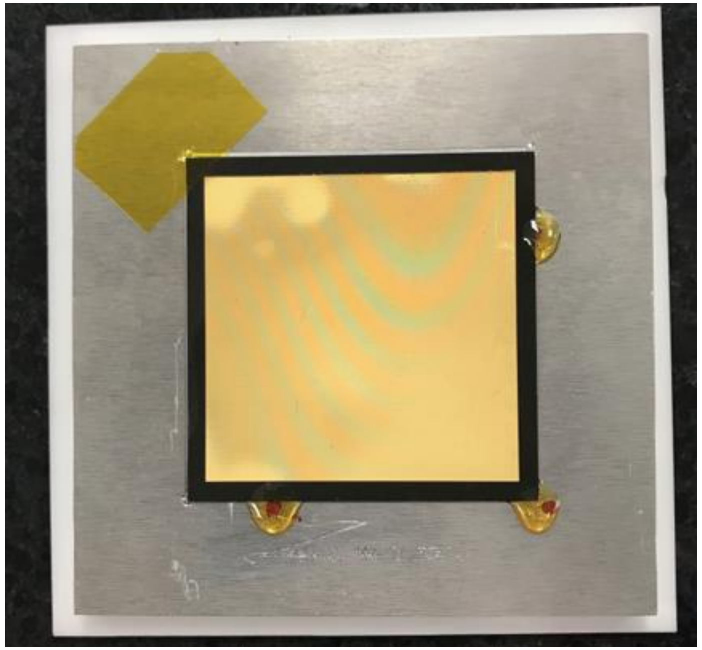

8k – 10k USD

Affordable

PCB printing

Decent quality, acceptable DF-DPC sensibility

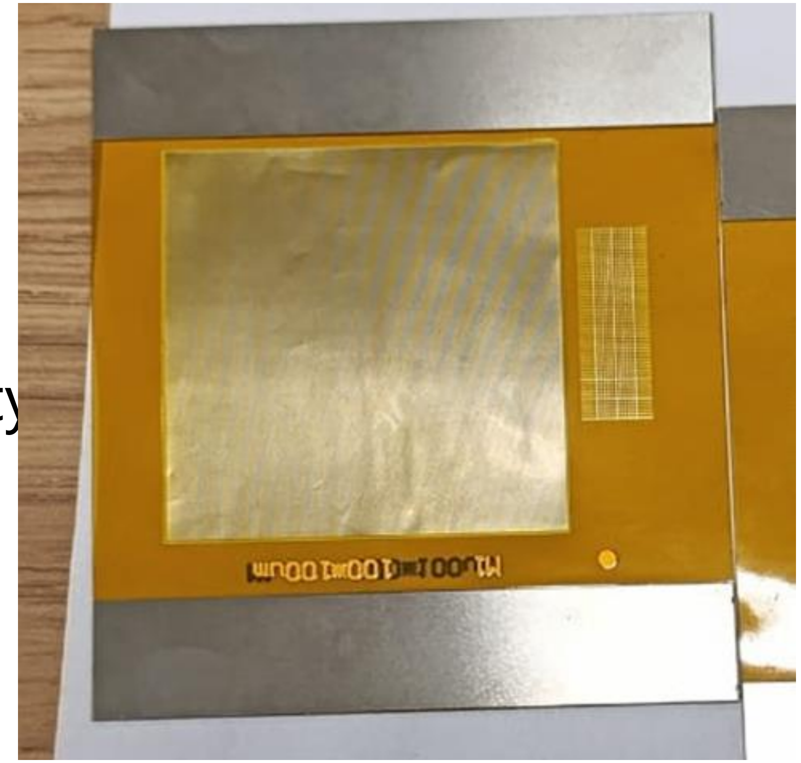

Conventional PCB printing >100um

Some imperfections

10 -14 USD

First prototype

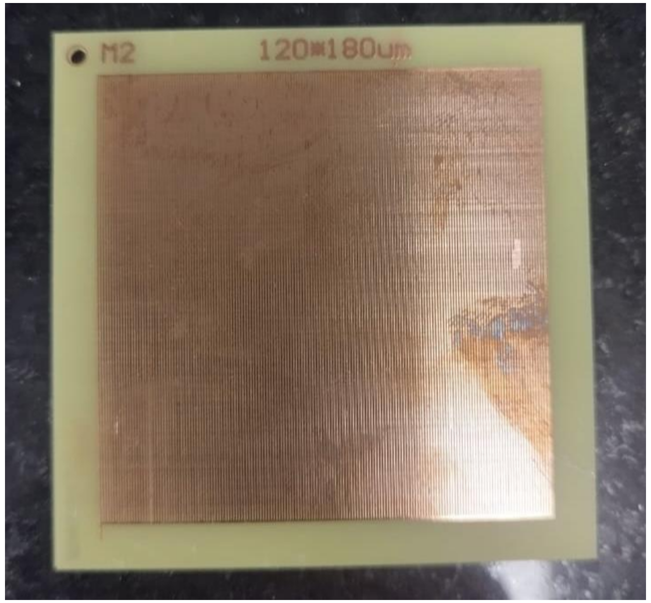

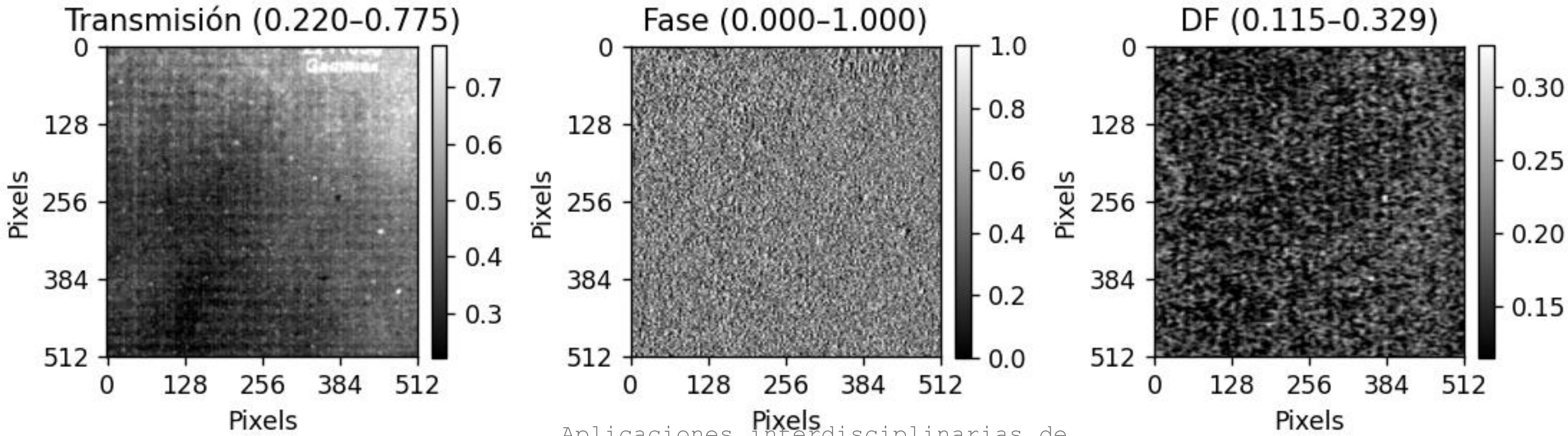

Second prototype

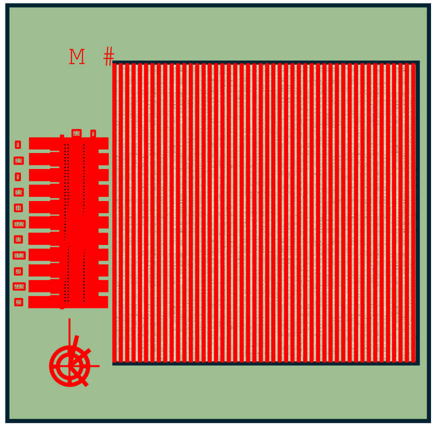

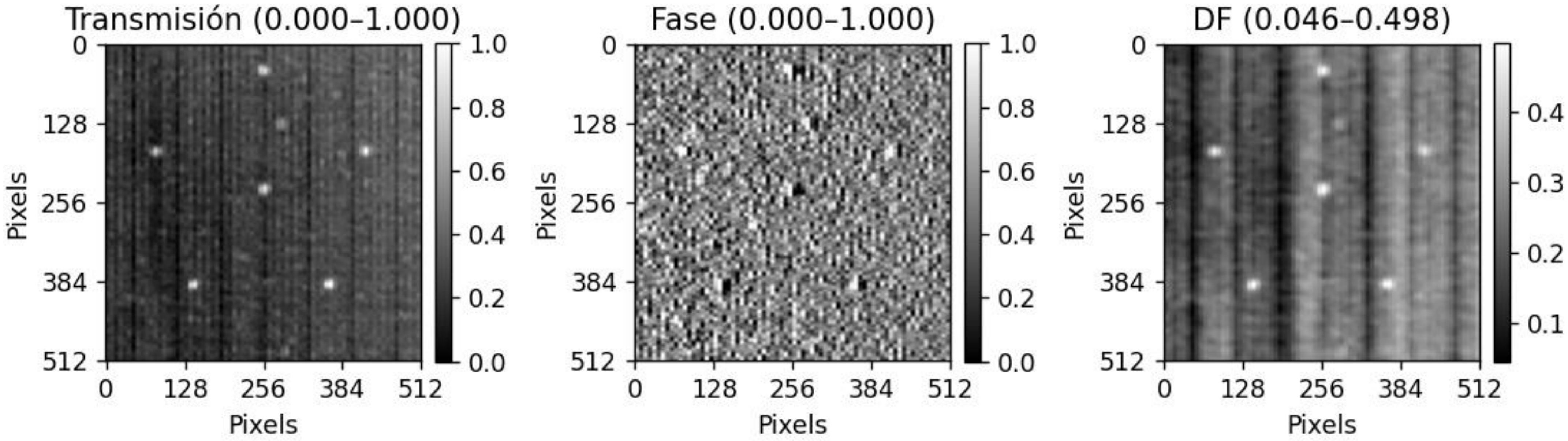

Third prototype

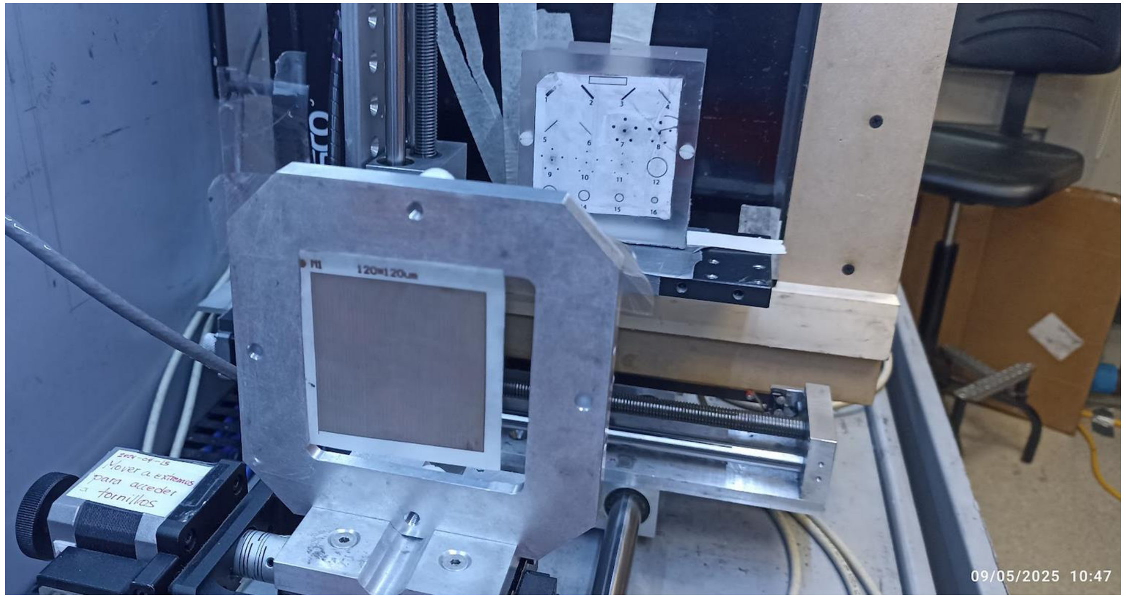

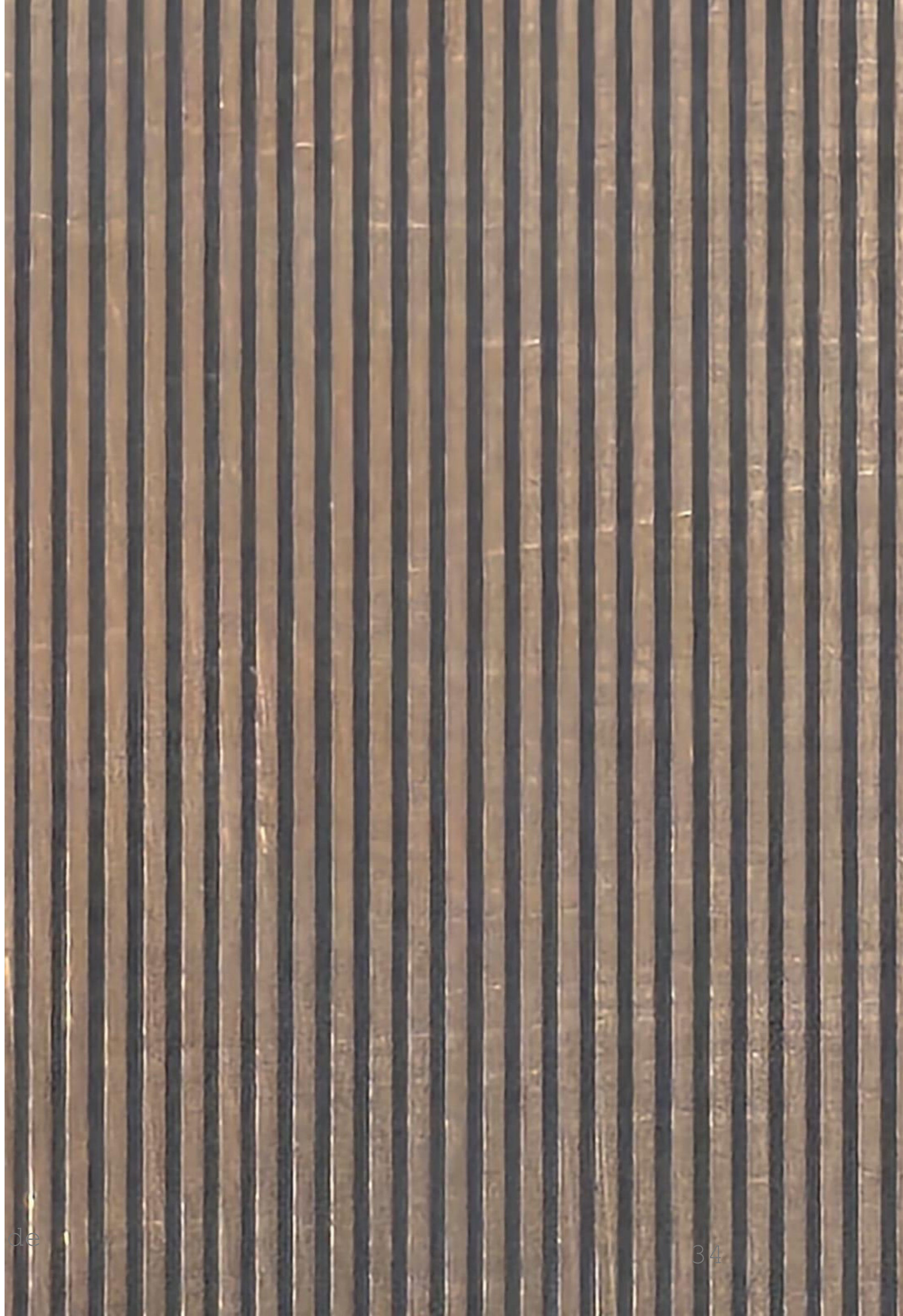

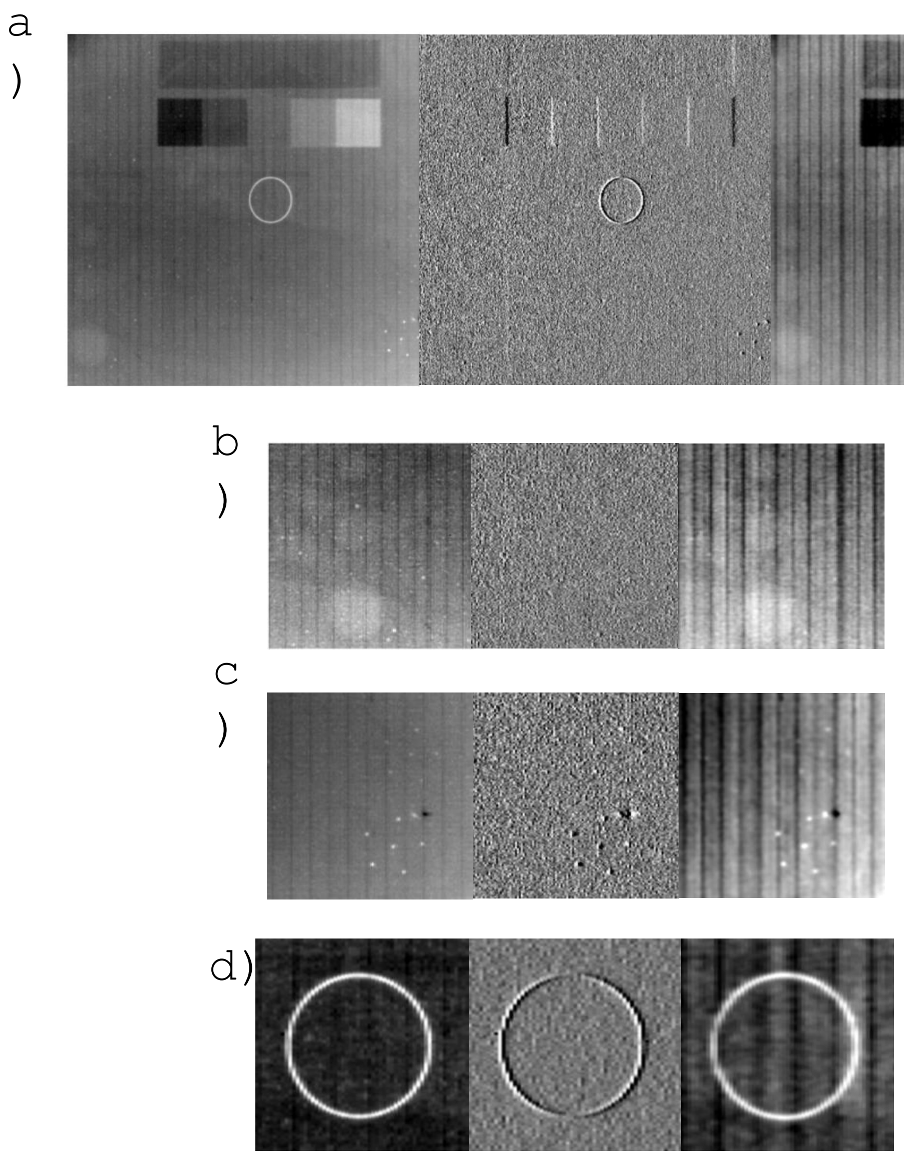
a)
b)
c)
d)

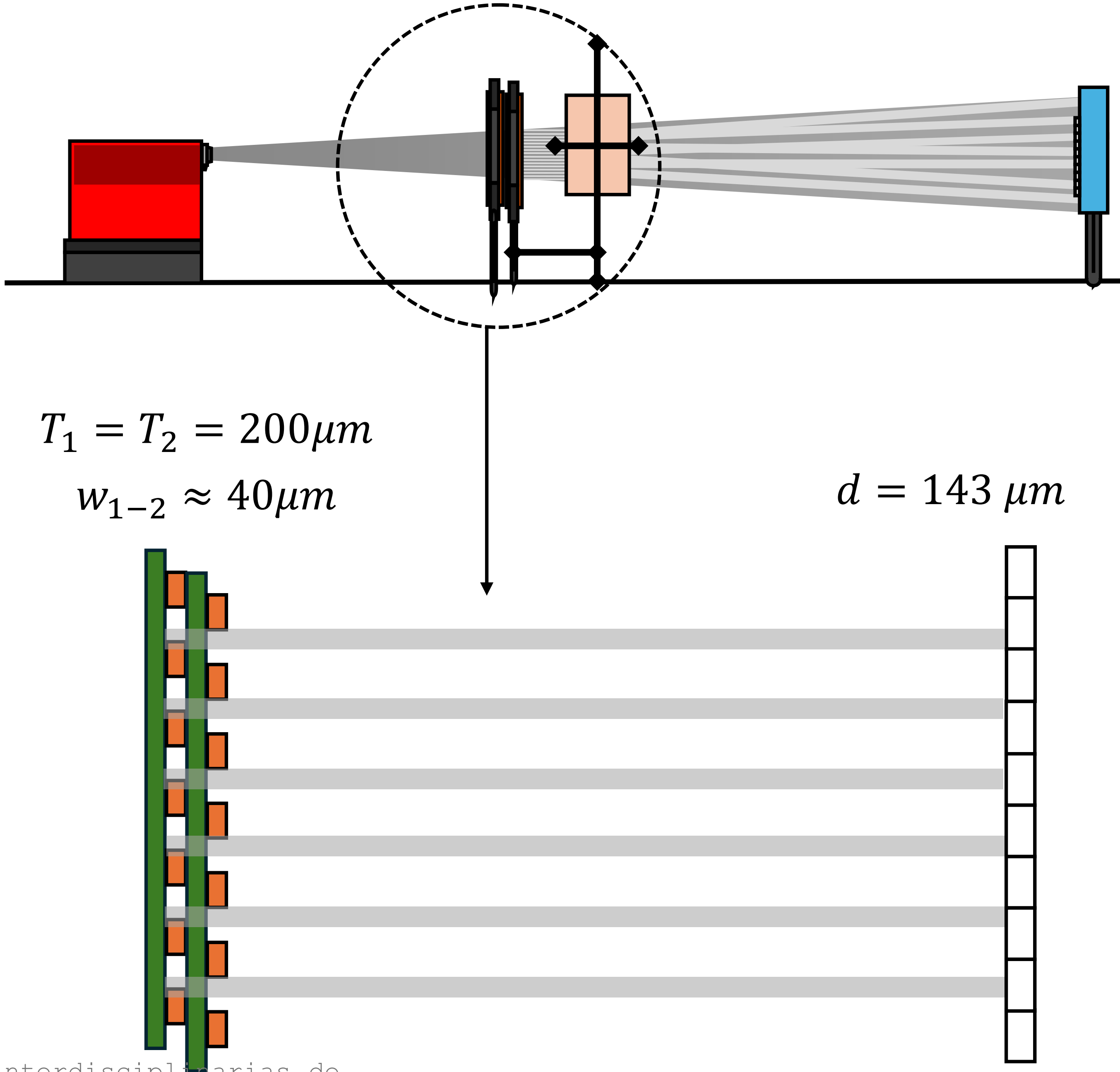
$T_1 = T_2 = 200\mu m$
$w_{1-2} \approx 40\mu m$
$d = 143\ \mu m$

Retrieval method

$$T_n(1 - L_n) = \frac{I_{n-1}^{(S)} + I_n^{(S)} + I_{n+1}^{(S)}}{I_{n-1}^{(M)} + I_n^{M} + I_{n+1}^{(M)}}$$

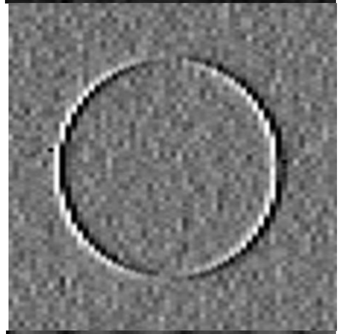

$$\frac{2\alpha_2}{w_e + \frac{1}{2}\alpha_1} D_n = \left(\frac{I_{n-1}^{(S)}}{I_{n-1}^{(M)}} - \frac{I_n^{(s)}}{I_n^{(M)}}\right) \frac{I_{n-1}^{(M)} + I_n^{M} + I_{n+1}^{(M)}}{I_{n-1}^{(S)} + I_n^{(S)} + I_{n+1}^{(S)}}$$

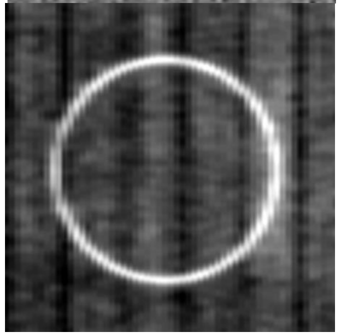

$$\frac{2\alpha_3}{w_e + 2\alpha_1} S_n = \left[1 - \frac{I_{n-1}^{(S)} + I_n^{(S)} - I_{n+1}^{(S)}}{I_{n-1}^{(M)} + I_n^{M} - I_{n+1}^{(M)}} \cdot \frac{I_{n-1}^{(M)} + I_n^{M} + I_{n+1}^{(M)}}{I_{n-1}^{(S)} + I_n^{(S)} + I_{n+1}^{(S)}}\right]$$

Do these masks work

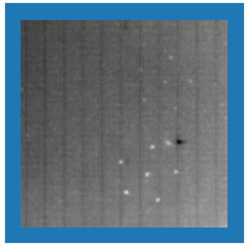

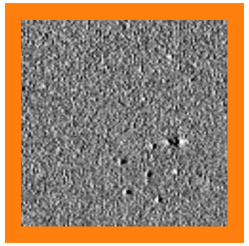

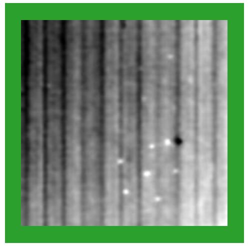

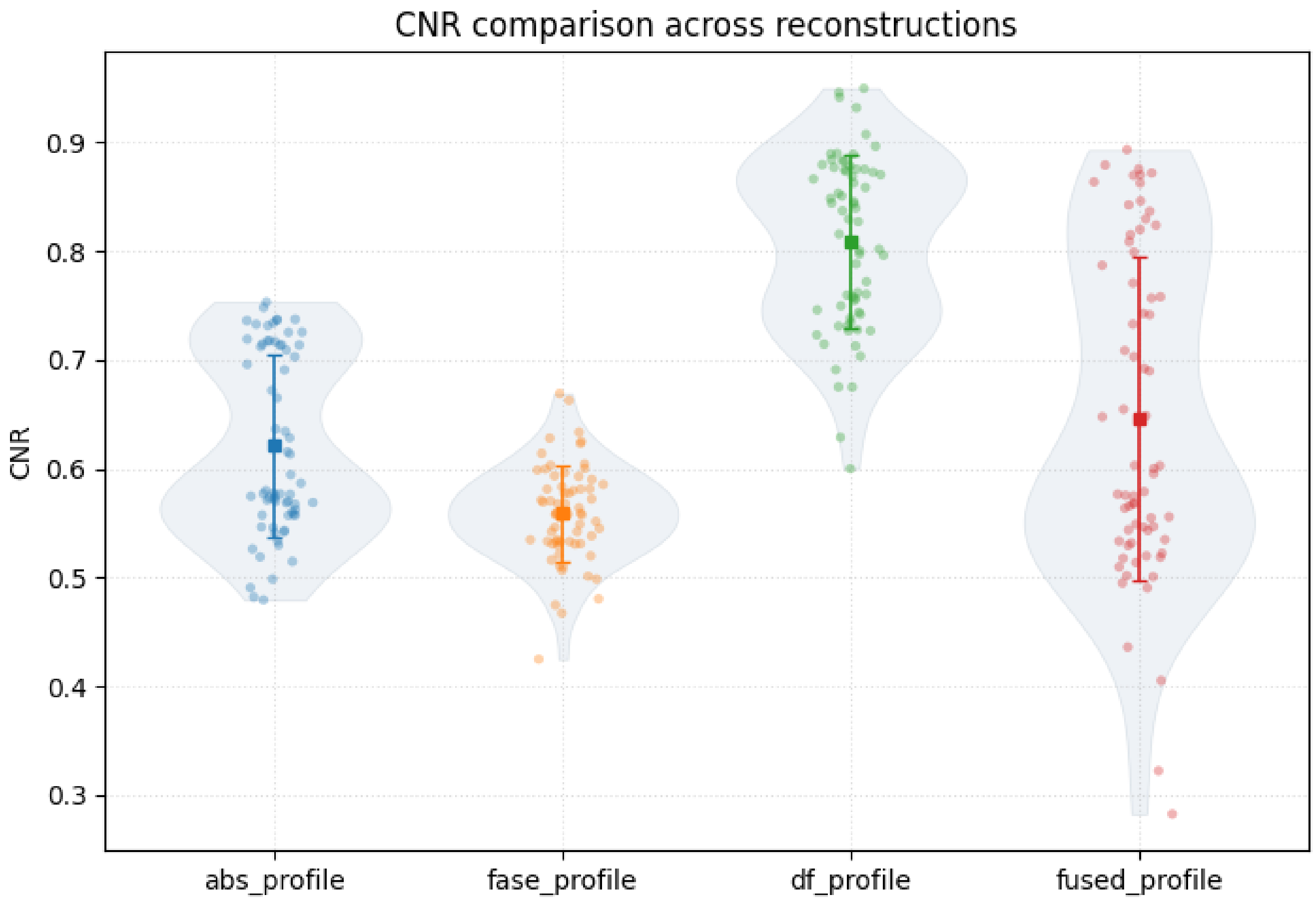

Final remarks

Mask modulation seems like a promising alternative to normalize DF-DPC imaging for several optical systems. Binning effects, dithering and artifacts are yet to be studied

PCB masks are a low-cost alternative that matches high-end photolythography masks for specific systems. A ground truth study is yet to be done to compare the effectiveness of PCB masks.

Bonus

This is a viable alternative for material classification (benign vs malignant microcalcifications)

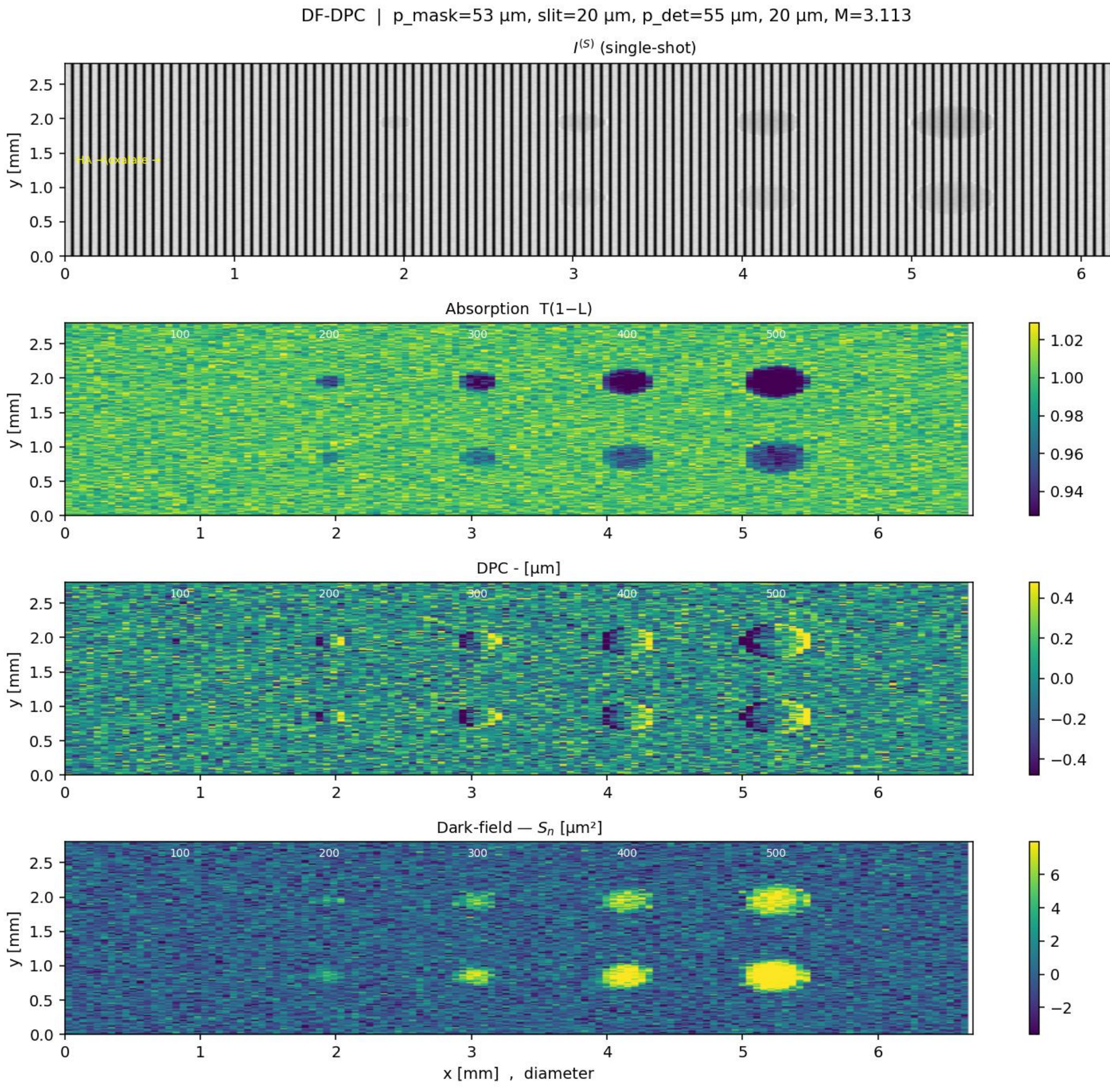

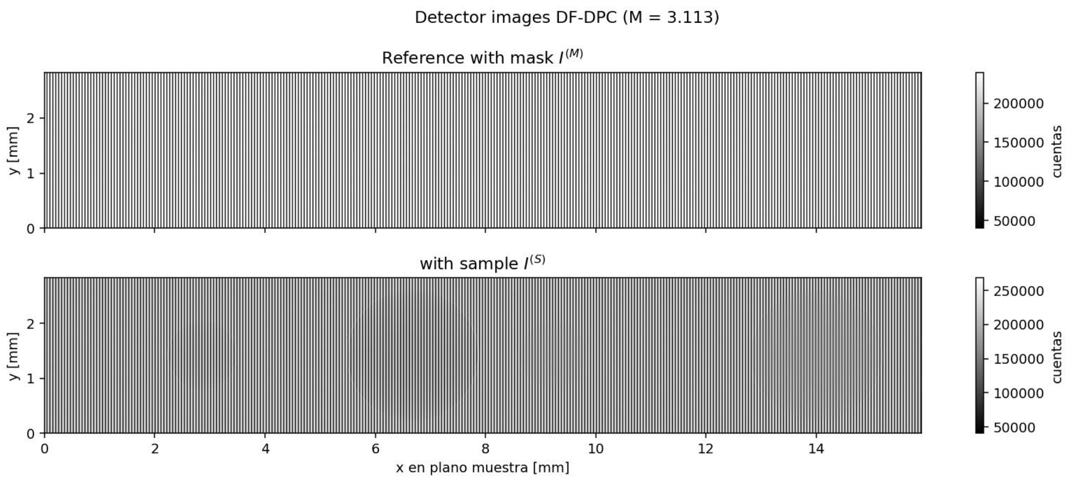
Detector images DF-DPC (M = 3.113)
Reference with mask $I^{(M)}$
with sample $I^{(S)}$
y [mm]
cuentas
x en plano muestra [mm]

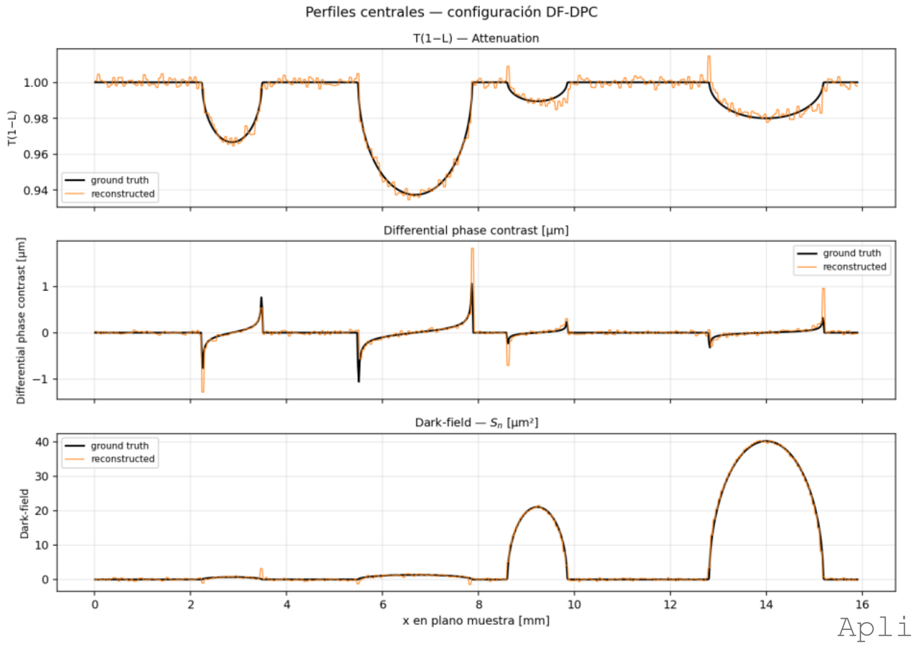
Perfiles centrales — configuración DF-DPC
T(1−L) — Attenuation
Differential phase contrast [µm]
Dark-field — S_n [µm²]
ground truth
reconstructed
Dark-field
x en plano muestra [mm]

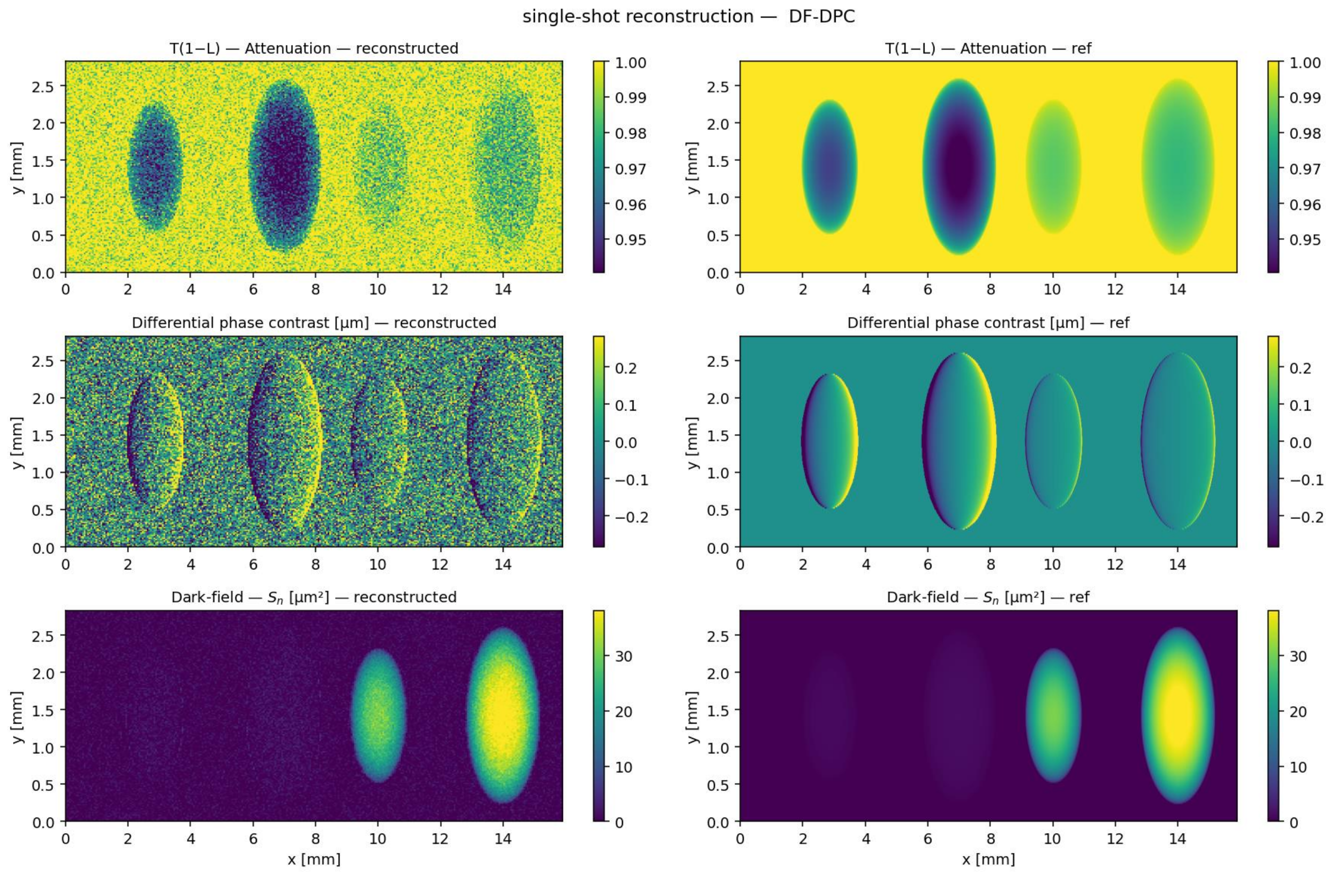
single-shot reconstruction — DF-DPC
T(1−L) — Attenuation — reconstructed
T(1−L) — Attenuation — ref
Differential phase contrast [µm] — reconstructed
Differential phase contrast [µm] — ref
Dark-field — S_n [µm²] — reconstructed
Dark-field — S_n [µm²] — ref
y [mm]
x [mm]

References

[1] Yuan, J., & Das, M. (2025). Single-shot, single-mask X-ray dark-field, and phase-contrast imaging. *Optica, 12*(12), 1895–1903. https://doi.org/10.1364/OPTICA.578430

[2] Paganin, D. M., & Morgan, K. S. (2019). X-ray Fokker–Planck equation for paraxial imaging. *Scientific Reports, 9*, Article 17537. https://doi.org/10.1038/s41598-019-52284-5

[3] Zuo, C., Li, J., Sun, J., Fan, Y., Zhang, J., Lu, L., Zhang, R., Wang, B., Huang, L., & Chen, Q. (2020). Transport of intensity equation: A tutorial. *Optics and Lasers in Engineering, 135*, Article 106187. https://doi.org/10.1016/j.optlaseng.2020.106187